Applied Catalysis B: Environmental 132–133 (2013) 90–97

Contents lists available at SciVerse ScienceDirect

Applied Catalysis B: Environmental

journal homepage: www.elsevier.com/locate/apcatb

# Potocatalytic oxidative degradation of organic pollutant with molecular oxygen activated by a novel biomimetic catalyst ZnPz(dtn-COOH)$_4$

Zehui Zhang, Mingjian Zhang, Jia Deng, Kejian Deng*, Bingguan Zhang, Kangle Lv, Jie Sun, Lianqing Chen

*Key Laboratory of Catalysis and Materials Sciences of the State Ethnic Affairs Commission & Ministry of Education, College of Chemistry and Material Science, South-Central University for Nationalities, Wuhan, 430074, China*

ARTICLE INFO

*Article history:*
Received 13 August 2012
Received in revised form 3 November 2012
Accepted 11 November 2012
Available online 29 November 2012

*Keywords:*
Zinc porphyrazine with sulfur
Biomimetic catalyst
Activating molecular oxygen
Photodegradation
Rhodamine B

ABSTRACT

Zinc porphyrins and its analogs showing many excellent properties such as good potosensitivity, non-toxicity, high stability and facile preparation attract more and more attention of scientists. Here, a novel zinc porphyrazine, namely zinc(II) tetracarboxyl- tetra(1,4-dithiin) porphyrazine [abbreviated as ZnPz(dtn-COOH)$_4$] was successfully synthesized and its potocatalytic activity was studied. The ZnPz(dtn-COOH)$_4$ supported on an Amberlite CG-400 resin was used as a biomimetic catalyst for the activation of molecular oxygen under visible light to degrade a probe dye compound Rhodamine B (RhB) in aqueous solution. Interestingly, the mechanism for the oxidative degradation of RhB involves both $^1O_2$ and HO$^\bullet$ (Type II and Type I mechanisms, respectively). More hydroxyl radicals were produced at pH 3, which was responded for the highest degradation ratio. The catalyst can be reused several times without losing its catalytic activity, with an average RhB degradation ratio around 80% for 12 h. The most probable mechanism of RhB degradation in this study was that N,N-diehyl-N-ethyl-rhodamine was the main intermediate, which was then cleaved to small molecule by reactive oxidizing species. This study demonstrated a promising approach for the activation of molecular oxygen by the newly developed biomimetic catalyst, in which the central metal to be unchangeable valence, for environmental remediation and oxidation catalysis.



## 1. Introduction

Organic dyes are widely used in a variety of technical applications, including dyeing of textiles, paper, plastics, or leather. Their variety, toxicity and persistence directly impact the health of ecosystems and present an immediate threat to human beings via contaminating drinking water supplies [1,2]. Therefore, it has become a challenge to achieve the effective removal of persistent organic pollutants from wastewater effluent to minimize pollution and to enable the water reuse.

There has been a significant amount of research on the removal of environmental pollutants. Various methods have been devoted to handle the dye removal from waste water including biological, physical and chemical methods [3–5]. The biological process takes place under mild conditions [6]. However, large-scale industrial application of these biological processes is difficult due to their inherent time-consuming procedure and their poor tolerance to organic contaminants. In addition, physical methods such as coagulation, adsorption, membrane filtration and ion exchange are employed to the removal of organic contaminants [7,8]. However, physical methods only transfer the contaminants from water phase, and large amounts of solid waste are also concomitant. Taking into account the disadvantage of biological and physical methods in the treatment of organic contaminants, there is still a pressing demand for developing economic and environmental-benign methods for the effective removal of organic pollutants from waste water. In recent years, advanced oxidation processes (AOPs) based on the generation of reactive species have been proposed to oxidize quickly and none selectively a broad range of organic pollutants [9–11]. Some typical technologies of AOPs have been successfully developed for the treatment of organic dyes, including UV/$H_2O_2$, Fenton schemes, semiconductor photocatalyst, and electrochemical catalysis.

Recently, biomimetic catalysis, which gathers the advantages of enzyme's recognition and chemical catalysis has attracted much attention [12]. Metalloporphyrins are well known for their electron-transfer roles in a myriad of redox systems in nature so as to have highly effective photocatalysts due to their very strong absorption in the 400–450 nm region (Soret band) and in the 500–700 nm region (Q-bands) [13]. Several synthetic metalloporphyrin derivatives with various structures and core metals have shown high potocatalytic activity and environmental-friendly to activate molecular $O_2$ or $H_2O_2$ in oxidation of organic compound and oxidative degradation of organic pollutants [14,15].

* Corresponding author. Tel.: +86 27 67843930; fax: +86 27 67842752.
*E-mail address:* dengkj@scuec.edu.cn (K. Deng).

0926-3373/$ – see front matter © 2012 Elsevier B.V. All rights reserved.
http://dx.doi.org/10.1016/j.apcatb.2012.11.027

Metalloporphyrazines (MPzs), with a structure similar to metalloporphyrins, exhibit a lot of excellent physical and chemical properties [16]. Among the MPzs, we recently found that iron tetra(1,4-dithiin) porphyrazines showed high photocatalytic activities for the oxidation degrade organic pollutants [17,18], and the mechanism was involved the electron transfer through center iron ion, due to the variable valence of iron ion. However, due to $Fe^{2+}$ is much more difficult to be chelated into porphyrazines, and this process often was carried out under harsh conditions and long reaction time. For all we know, zinc porphyrins and its analogs showing excellent properties such as good potosensitivity, high stability, non-toxicity and facile preparation have been favored by scientists. Particularly, their attractive photo-sensitivity to conduce the magnitude of singlet oxygen quantum yield which was used for the photo-splitting water, photodynamic therapy and photocatalytic oxidation of organic compounds [19]. These excellent properties prompted us to design a facile prepared zinc sulfur-containing porphyrazine to study its potocatalytic oxidative degradation of organic pollutants. At the same time, considering the hydrophilicity of the zinc complex, four carboxylic groups were introduced onto the periphery of its large ring. In this paper, a novel biomimetic photocatalyst zinc porphyrazine bearing tetracarboxylic-tetra(1,4-dithiin) groups [abbreviated as $ZnPz(COOH)_4$] was synthesized, and its photocatalytic activity of the activation of molecular oxygen to oxidation degradation of Rhodamine B (RhB) was studied under visible light irradiation in an aerated suspension.

## 2. Experimental

### 2.1. Materials and methods

The disodium dithiomaleonitrile salt (Scheme 1, Compound 1) was prepared according to the previously reported procedures [20]. 2,2,6,6-Tetramethylpiperidine (TMP) was purchased from Sigma–Aldrich. All reagents and solvents were obtained from commercial suppliers (Wuhan Guoyao Chemical Reagent Co., Ltd.,) with reagent grade quality. Doubly distilled water was used throughout this study.

### 2.2. Synthesis of 2,3-dicyano-5-methyl formate-1,4-dithiin (Compound 3)

Methyl 2,3-dibromopropionate 2 (7.8 g, 32 mmol) was added dropwise into a mixture of disodium dithiomaleonitrile salt (1) (6.0 g, 32 mmol) in ethylene glycol dimethyl ether (60 mL) at 70 °C, and stirred vigorously for 48 h under a nitrogen atmosphere. After reaction, solvent was removed under reduced pressure. The crude residue was washed with water and extracted with $CH_2Cl_2$. Then $CH_2Cl_2$ was removed to give crude product, which was purified on a silica column with petroleum ether:ethyl acetate (1:3, v/v) as eluent to obtain 1.19 g compound 3 in a yield of 23.9%. IR (KBr, $cm^{-1}$): 2953, 2857, 1442 for (C—H) $CH_3$; 2924 for (C—H) $CH_2$; 2227 for C≡N; 1739 for C=O; 1638, 1513, 1378 and1318 for C=C; 1278 and 1164 for C—C; 1261 for C—O; 1042 and 805 for C—S; $^1H$ NMR (400 MHz, $CDCl_3$, ppm): 3.95, 4.40 (d, 2H, S—$CH_2$—), 3.85 (s, 3H, —$CH_3$), 3.52 (t, 1H, S—CH—). MS ($m/z$) = 226.32 $[M]^+$.

### 2.3. Synthesis of tetra(1,4-dithiin) porphyrazine magnesium (II) bearing peripheral tetramethyl formate (Compound 4)

Firstly, magnesium butoxide solution was prepared by the reaction of magnesium turnings (0.125 g, 5.21 mmol) with *n*-butanol (20 mL) with a small chip of iodide as catalyst under reflux for 18 h. Then, a solution of compound 3 (0.76 g, 3.36 mmol) in chlorobenzene (20 mL) was added dropwise into the above magnesium butoxide solution for 1 h, and the mixture was stirred for 24 h under reflux. After reaction, solvents were removed to give a solid residue. The crude residue was primarily purified by washing several times with methanol until filter liquor being colorless, which was further purified on a silica column with chloroform:methanol (60:1, v/v) as eluent. Compound 4 (0.168 g) was obtained in a yield of 21.5%. IR(KBr, $cm^{-1}$) $\nu$: 2956, 2870 for (C—H) $CH_3$; 2932 for (C—H) $CH_2$; 1730 (C=O), 1261 for C-O; 1616, 1500(C=C), 1465, 1379, 1300 are assigned to the macrocyclic skeleton of the C—N and the C=N; 1268 and 1160 for C—C; 1049, 803 for (C—S). UV–vis [chloroform, $\lambda_{max}$/nm]: Q band with $\lambda_{max}$ 656 and 520 nm; B band with $\lambda_{max}$ 367 nm. MS ($m/z$) = 929.45 $[M]^+$. The XPS spectrum showed the presence of the 2P Mg(II) iron peaks with a binding energy of 53.32 eV.

### 2.4. Synthesis of metal-free porphyrazine (Compound 5)

A solution of compound 4 (0.08 g, 0.086 mmol) in 5 mL of trifluoroacetic acid was stirred for 12 h at room temperature in dark, then the solution was poured into ice water to precipitate the target compound. The solid residue was washed with ammonia solution (10%), deionized water and methanol in sequence. The dark purple product was purified on silica gel using chloroform/ethanol (40:1, v/v) as eluent to get 0.06 g metal free porphyrazine (compound 5) in a yield of 78.1%. IR (KBr, $cm^{-1}$): 3288 (N—H), 2961, 2854 for (C—H) $CH_3$; 2923 for (C—H) $CH_2$; 1727 (C=O), 1264 for C—O; 1632, 1461, 1382, for the macrocyclic skeleton; 1270 and 1174 for C—C; 1050, 802 for (C—S). UV-vis [chloroform, $\lambda_{max}$/nm]: Q band with $\lambda_{max}$ 698, 622 and 524 nm. B band with $\lambda_{max}$ 352 nm. MS ($m/z$) = 907.11 $[M]^+$.

### 2.5. Synthesis of Zn(II) porphyrazine (Compound 7)

$Zn(OAc)_2.2H_2O$ (0.24 g, 1.10 mmol) and metal-free porphyrazine (compound 5) (0.10 g, 0.11 mmol) were added into a mixture solution of ethanol (7 mL) and chloroform (15 mL), and the mixture was stirred for 10 h at reflux temperature. Then solvents were removed, and the residue was washed with water and diethyl ether in sequence until the filter liquor was colorless. The product was purified on silica gel with chloroform/ethanol (50:1, v/v) as eluent to give compound 6 in a yield of 59.2%. Compound 6 was firstly dissolved in 20 mL dichloromethane, and then 50 mL 0.5 mol/L NaOH was added. The hydrolysis of compound 6 was carried out at 50 °C for 3 h. After reaction, the reaction mixture was filtered, and it was washed with 5% HCl aqueous solution repeatedly until the pH of filtrate is 3. Then the crude product was washed with water and ethanol in sequence. Finally, compound 7 was extracted with chloroform from the above crude product in a yield of 54.0%. IR(KBr, $cm^{-1}$) $\nu$: 3545 for (—COOH), 2925 for (C—H) $CH_2$; 1622 (C=O), 1254 for C—O; 1630, 1505 (C=C), 1468, 1389, 1305 are assigned to the macrocyclic skeleton of the C—N and the C=N; 1254 and 1151 for C—C; 1050, 802 for (C—S). UV–vis [DMF, $\lambda_{max}$/nm]: Q band with $\lambda_{max}$ 659 and 525 nm; B band with $\lambda_{max}$ 375. MS ($m/z$) = 914.40 $[M]^+$. XPS spectra indicated the presence of the $2P_{1/2}$ Zn(II) peaks with a binding energy of 1043 eV and $2P_{3/2}$ with a binding energy of 1021 eV.

### 2.6. Preparation of CG-400 resin supported $ZnPz(COOH)_4$ ($ZnPz(COOH)_4$/resin)

5.0 mg $ZnPz(COOH)_4$ was firstly dissolved in 100 mL DMSO under ultrasonic action. Then the solution was added dropwise into 100 mL distilled water containing 1.0 g activated Amberlite CG-400 anion-exchanged resin under stirring for 24 h. The resin supported $ZnPz(COOH)_4$ was formed. The suspension was filtrated under reduced pressure and washed three times with water, then dried at 40 °C for 24 h. The loading amount of $ZnPz(COOH)_4$ on the resin was calculated by the change of UV–vis absorbance of

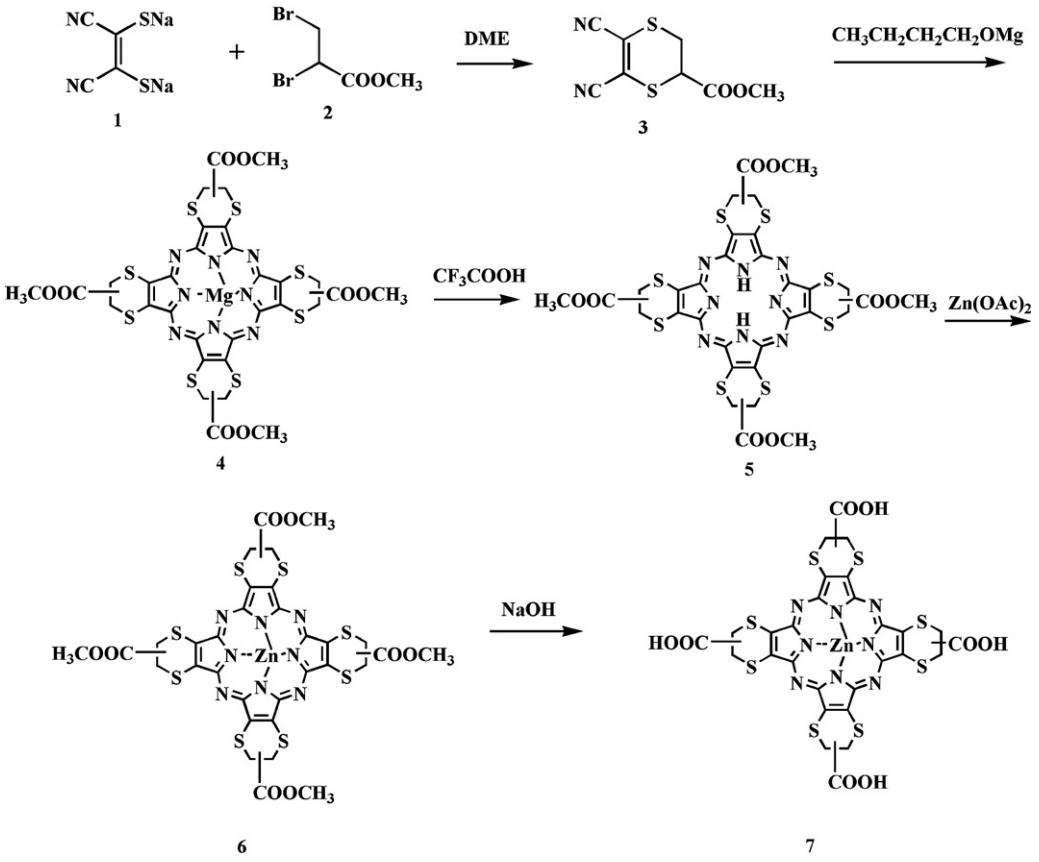


**Scheme 1.** Scheme illustration for the synthesis of ZnPz(dtnCOOH)$_4$.

ZnPz(COOH)$_4$ in the mixed solution before and after adsorption of the resin, and the content of ZnPz(COOH)$_4$ was equal to 4.0‰.

### 2.7. Photocatalytic degradation of RhB catalyzed by ZnPz(COOH)$_4$/resin

40 mg ZnPz(COOH)$_4$/resin was added into 50 mL RhB ($2 \times 10^{-5}$ mol/L), and the mixture was stirred for an additional 12 h in dark before light irradiation. Then the suspension containing the catalyst and RhB was irradiated by a 500 W halogen lamp with a filter cutoff ≤420 nm wavelength light in an aerated suspension for 12 h, during which the degradation of RhB was determined from the changes in absorbance on samples obtained at different irradiating intervals.

### 2.8. HPLC analysis of degradation products of RhB

Analysis of the degradation products of RhB was done on a VARIAN ProStar 210 HPLC system. The samples were separated using a reversed-phase C18 column (200 × 4.6 mm) at 500 nm. The column temperature was maintained at 30 °C. The optimized mobile phase consisted of methanol and water with the volume ratio at 70:30. The flow rate was set at 1.0 mL/min.

### 2.9. The cyclic voltammetry (CV) measurement of ZnPz(dtnCOOH)$_4$ and its free base

The measurements were carried out with electrochemistry workstation controlled by an external PC and utilizing a three-electrode configuration at room temperature. The working electrode was a Pt disc with a diameter of 2 mm. The surface of the working electrode was polished with $Al_2O_3$ suspension before each run. A Pt wire served as the counter electrode. Saturated calomel electrode (SCE) was employed as the reference electrode and separated from the bulk of the solution by a glass bridge. A solution of 0.10 mol/L tetrabutylammonium perchlorate (TBAP) in extra pure DMF was employed as the supporting electrolyte. High purity $N_2$ was used to remove dissolved $O_2$ at least 15 min prior to each run and to maintain a nitrogen blanket during the measurements.

### 2.10. Determination of active species by electron paramagnetic resonance technology

Electron paramagnetic resonance (EPR) investigations were carried out on a Brucker model EPR 300E spectrometer, which was equipped with a Quanta-Ray Nd:YAG laser (532 nm). TMP was used as the spin-trapping reagents to detect singlet oxygen ($^1O_2$). The EPR spectrometer was coupled to a computer for data acquisition and instrument control. All of the measurements were carried out at room temperature.

## 3. Results and discussions

### 3.1. Synthesis and characterization

The starting point of ZnPz(COOH)$_4$ is 2, 3-dicyano-5-methylformate-1,4-dithiin (compound 3), which was obtained from the reaction of disodium dithiomaleonitrile salt (compound 1) with 2,3-dibromopropan-1-methylformate (compound 2) (Scheme 1). The blue-green magnesium porphyrazine (compound 4) was obtained in a yield of 21.5% via the template reaction of dinitrile derivative (compound 3) with magnesium butoxide. Compared the IR spectra of compound 4 with 3, the disappearance of C≡N peak at 2237 cm$^{-1}$ in compound 4 was an convinced proof

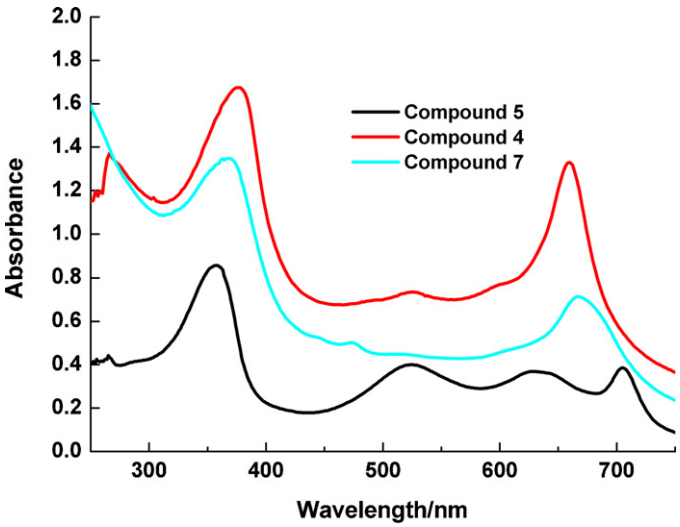


**Fig. 1.** UV–vis spectra of compound 4, 5 and compound 7 in DMF.

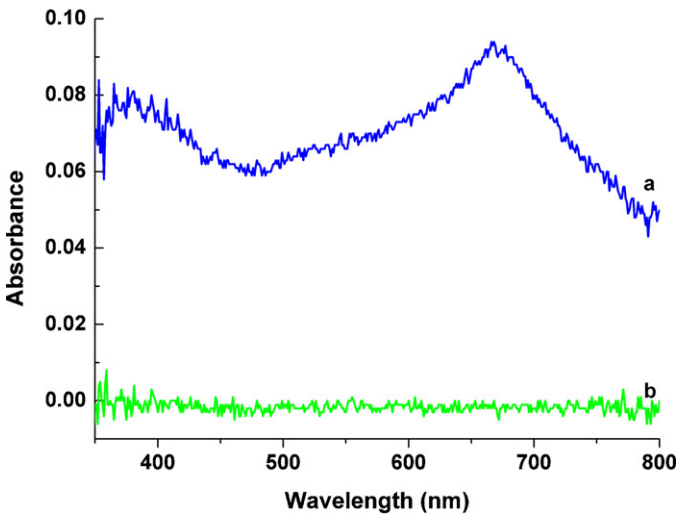


**Fig. 2.** Diffuse reflectance spectra of the samples. (a) ZnPz(dtnCOOH)4 supported on CG-400 resin, (b) the resin, respectively.

of the cyclotetramerization of compound 3. Treatment of this magnesium porphyrazine (compound 4) with triflouroacetic acid afforded the metal-free porphyrazine (compound 5). Apparent differences between magnesium and metal-free porphyrazine are the change of color from the dark blue–green to purplish blue. The IR peak at 3288 $cm^{-1}$ is the N—H stretching vibration of metal-free porphyrazine, indicating that the metal magnesium was successfully removed. On the other hand, UV–vis absorption spectra are also an important method for identification of metal or metal-free porphyrazine. The first intense band of porphyrazine core is dominated by Q-band, which is always observed between 648 and 680 nm due to $\pi \rightarrow \pi^*$ transition. A second intense and broad $\pi \rightarrow \pi^*$ transition in near UV region of 343–380 nm called soret or B-band is also a characteristic of these tetrapyrole derivatives [21,22]. As shown in Fig. 1, magnesium porphyrazine exhibits a strong Q band at 660 nm and a strong B band at 367. Incidentally, a weak absorption band around 526 nm is observed due to the $n \rightarrow \pi^*$ transitions of peripheral sulfur atoms and macrocyclic $\pi$ system [23]. As expected, metal-free porphyrazine shows a splitted Q-band at 704 and 630 nm because of the change of symmetry of magnesium porphyrazine core from $D_{4h}$ in the case of metallo-species to $D_{2h}$ in the metal-free porphyrazine [24].

Coordination of $Zn^{2+}$ into metal-free porphyrazine was carried out by the reaction of $Zn(OAc)_2$ with metal-free porphyrazine (compound 5) at reflux temperature, giving rise to compound 6 in a yield of 59.2%. Hydrolysis of compound 6 was catalyzed by an aqueous solution of 0.5 mol/L NaOH at 50 °C. The final product $ZnPz(dtnCOOH)_4$ (compound 7) was obtained in a yield of 54.0%. XPS spectra indicated the presence of the $2P_{1/2}$ Zn(II) peaks with a binding energy of 1043 eV and $2P_{3/2}$ with a binding energy of 1021 eV. UV-Vis spectra of $ZnPz(dtnCOOH)_4$ showed a Q-band at 659 nm as expected from $D_{4h}$ symmetry and a B-band at 375 nm (Fig. 1), indicating $Zn^{2+}$ was introduced into porphyrazine core. IR spectra also indicated that the $Zn^{2+}$ was inserted into the metal-free porphyrazine core, due to the disappearance of N-H stretching vibration band at 3288 $cm^{-1}$. Mass spectra analysis with $[M]^+$ to be 914.40 was in accordance with the proposed structure of $ZnPz(dtnCOOH)_4$. Compared with precursors tetra(1,4-dithiin)porphyrazin, the solubility of $ZnPz(dtnCOOH)_4$ is largely improved by introducing four carboxylic acids groups into its periphery. It is very soluble in common polar organic solvents such as DMSO, DMF. A good solubility is beneficial for its utilization in various fields.

### 3.2. Diffuse UV–vis reflectance spectrum of $ZnPz(dtnCOOH)_4$/CG-400 resin

One of the serious problems encountered is the photo-inactive dimerized species formed in solutions when using metal porphyrazines and its analogs for activation of molecular oxygen [25]. One important method of preventing the formation of dimers is to load porphyrazines and its analogs onto the surface of support. In addition, the supported catalysts can facilitate catalyst separating and recycling. Due to the strong interaction between the lone pair electrons on sulfur atoms in catalyst with anion exchange resin, Amberlite CG-400 resin was selected as a support for the immobilization of $ZnPz(dtnCOOH)_4$. The diffuse reflectance spectra of $ZnPz(dtnCOOH)_4$/CG-400 is shown in Fig. 2. An absorption band around 660 nm was observed for $ZnPz(dtnCOOH)_4$/CG-400 (Fig. 2, curve a), which was similar to the Q-band observation for $ZnPz(dtnCOOH)_4$ in DMF solution (Fig. 1). However, there was no absorption band for CG-400 resin (Fig. 2, curve b). These results clearly indicated that $ZnPz(dtnCOOH)_4$ was successfully immobilized on CG-400 resin by the electrostatic interaction.

### 3.3. Potocatalytic degradation of RhB catalyzed by $ZnPz(dtnCOOH)_4$/CG-400 resin

Prior to photocatalytic degradation of RhB, adsorption equilibrium was carried out over $ZnPz(dtnCOOH)_4$/CG-400 until the absorbance of RhB at 553 nm in UV-Vis spectra was kept changeless. Firstly, the degradation of RhB was carried out in an aerated suspension with air in the presence of $ZnPz(dtnCOOH)_4$/resin under visible light irradiation at pH 3, and the UV–vis absorption spectra of the RhB at various intervals are shown in insert of Fig. 3. The characteristic absorbance of RhB at 553 nm decreased continuously during the irradiation process. RhB was effectively degraded by 82% for 12 h. Compared with our previous results, the synthesized iron(II) tetramethyl-tetra(1,4-dithiin) porphyrazine [denoted as $Fe(II)Pz(Me\text{-}dtn)_4$] and iron(II) tetra(1,4-dithiin) porphyrazine bearing peripheral tetrapropyl-bromine [denoted as $Fe(II)Pz(BrPr\text{-}dtn)_4$] were used as catalysts, and about 78% and 70% of the RhB were degraded in the presence of $Fe(II)Pz(Me\text{-}dtn)_4$ and $Fe(II)Pz(BrPr\text{-}dtn)_4$ under light irradiation in an aerated suspension with air for 27 h and 24 h, respectively [17,18]. The degradation efficiency of RhB in the presence of $ZnPz(dtnCOOH)_4$ was much better than our previous results though the valance of center metal iron

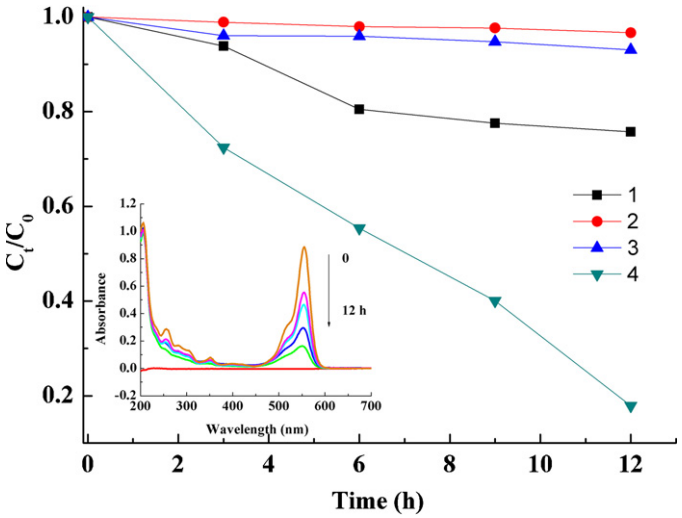


**Fig. 3.** Control experiments on the photocatalytic degradation of RhB at pH 3. Insert is the UV-Vis absorption spectra of the RhB at various intervals during the degradation process with air, light and catalyst. (1) with air and light, without catalyst; (2) with $N_2$, catalyst, and light; (3) with air and catalyst, without light; (4) with air, light and catalyst.

atom in their catalysts is variable, which is generally considered to facilitate the transfer of electrons.

It was noted that absorbance of RhB at 553 nm did not undergo any wavelength shift. The result indicated that the conjugated xanthene ring in RhB was firstly cleaved to form smaller fragments without successive de-N-ethylation [26].

Control experiments on the photocatalytic degradation of RhB are shown in Fig. 3. No significant degradation of RhB was observed under suspension aerated with $N_2$ (Fig. 3, curve 2). It indicated that molecular oxygen was the oxidant in the oxidation degradation of RhB. It was also noted that RhB could not be degraded in dark in the presence of oxygen and catalyst (Fig. 3, curve 3). It indicated that light irradiation was necessary for the formation of reactive oxidation species. However, a small amount of RhB with 24% was degraded with oxygen and light irradiation, even in the absence of catalyst (Fig. 3, curve 1), and it may be attributed to self-photosensitized oxygenation of RhB through singlet oxygen [27]. All these results indicated that oxygen, light irradiation and ZnPz(dtnCOOH)$_4$/resin catalyst were very crucial for the effective degradation of RhB.

### 3.4. The effect of pH on the potocatalytic degradation of RhB catalyzed ZnPz(dtnCOOH)$_4$/CG-400 resin

It is known that pH value is an important operational variable in actual wastewater treatment. Thus the photocatalytic degradation of RhB catalyzed by ZnPz(dtnCOOH)$_4$/resin was carried out at different pH, and the results were shown in Fig. 4. It is clearly observed that pH has a notable effect on the degradation efficiency. The degradation efficiency of RhB was decreased in an order of acidic, alkaline conditions and neutral conditions, and the ratio of degraded RhB were 82%, 54%, and 34%, respectively. It would be interesting to explore why the degradation of RhB was much more effective in acidic conditions. It is reported that the adsorption of RhB on the catalyst surface is an important parameter to affect the degradation efficiency [28]. During our absorption equilibrium experiments, the results demonstrated that the amount of RhB adsorbed on the catalyst surface were almost the same around 15% at different pH. Thus adsorption ability of RhB on the catalyst surface should be excluded from relation with the highest degradation efficiency in acidic solutions. Therefore, taking account into

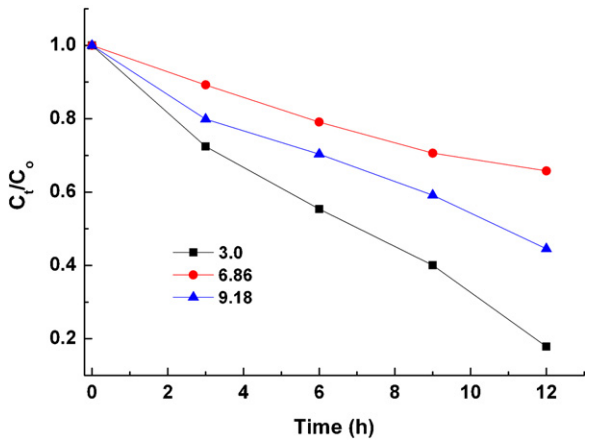


**Fig. 4.** The effect of pH values of RhB on its photocatalytic degradation.

the mechanism of degradation would be easy to understand the difference in the catalytic activity at different pH.

### 3.5. Possible mechanism for the potocatalytic oxidative degradation of RhB in the presence of ZnPz(dtnCOOH)$_4$/resin

In our previous work, it was found that hydroxyl radicals (HO•) were the main reactive oxidizing species (ROS) during the degradation of RhB with $H_2O_2$ as oxidant and iron (II) porphyrazine as catalyst, which was involved two mechanisms, namely electron transfer of the center metal iron similar to Fenton reaction and the oxidative performance of high-valence iron-oxo species [17]. Unlike the central iron ion in iron (II) porphyrazine, the valence state of the central zinc(II) in ZnPz(dtnCOOH)$_4$ is unchangeable. Therefore, the central zinc in ZnPz(dtnCOOH)$_4$ could not occur the electron transfer to produce ROS such as HO• or the high valance state zinc-oxo species. Like most cases of Zn porphyrins (ZnPrs) and Zn phthalocyanine (ZnPcs) as photosensitizers to activate $^3O_2$ into active $^1O_2$ under light irradiation [29], so does the zinc porphyrazine (ZnPz) for its structure similar to ZnPr and ZnPc.

In order to detect the possibility of generating singlet oxygen species during the degradation process, an electron paramagnetic resonance (EPR) spin-trapping method was used, and TMP was employed as the spin-trapping reagent. Fig. 5 presents the EPR

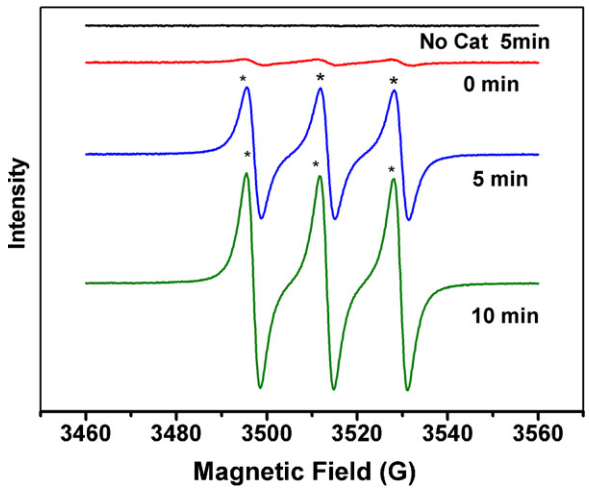


**Fig. 5.** EPR spectra of TMP adduct with $^1O_2$ generated in the potocatalytic degradation of RhB process. Reaction conditions: 40 mg ZnPz(COOH)$_4$/resin was added into 50 mL RhB ($2 \times 10^{-5}$ mol/L) pH at pH 6.86, then 20 μL TMP was added in an aerated suspension with oxygen.

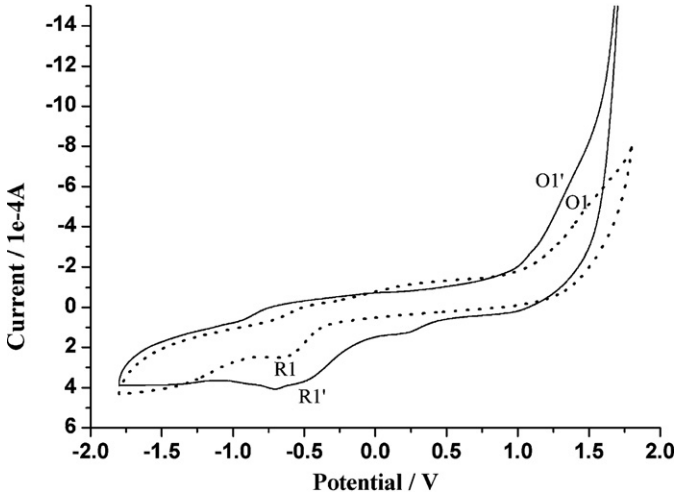


**Fig. 6.** The cyclic voltammogram of the ZnPz(dtnCOOH)$_4$ complex 7 (solid line) and its free base (dot line).

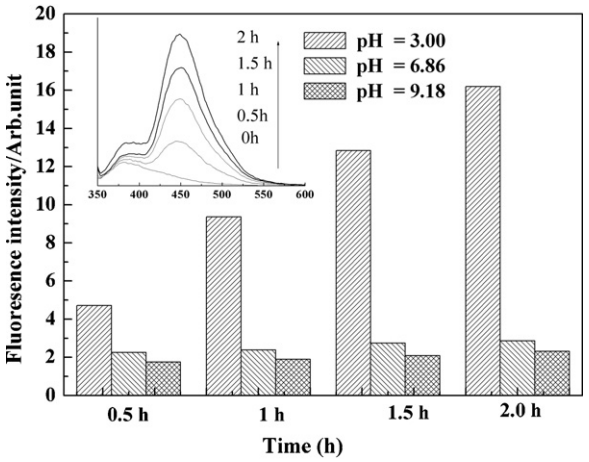


**Fig. 7.** Fluorescence intensities during the light-irradiation process through the capture of HO$^\bullet$ by coumarin with ZnPz(dtnCOOH)$_4$/resin at different pH. The insert shows the fluorescence intensity change during the light-irradiation process through the capture of HO$^\bullet$ by coumarin in pH 3 with ZnPz(dtnCOOH)$_4$/resin.

spectra of the spin adduct of $^1O_2$ and TMP with pulsed laser illumination at $\lambda = 532$ nm at pH 6.86. It can be seen that, a characteristic 1:1:1 triplet EPR signal, which is typically attributed to the EPR spectrum of the spin adduct of $^1O_2$ and TMP, is detected. It was also noted that the intensity of signals was increased during 0–15 min under light irradiation. As a control experiment, no ZnPz(dtnCOOH)$_4$ was added, no signal was detected. The results clearly indicated that $^1O_2$ could be generated in the presence of ZnPz(dtnCOOH)$_4$.

As far as the mechanism of the formation of $^1O_2$ catalyzed by ZnPz(dtnCOOH)$_4$ under light irradiation. It can be described as follows. Briefly, ZnPz are irradiated under light irradiation and get excited to the single state ($^1$ZnPz*), which then undergoes intersystem crossing to the triplet state ($^3$ZnPz*). This triplet state then interacts with ground (triplet) state molecular oxygen ($^3O_2$) generating excited singlet oxygen ($^1O_2$), which subsequently oxidizes the substrate by the following mechanism (called type II mechanism);

$$\mathrm{ZnPz} \xrightarrow{h\nu} {}^1\mathrm{MPz}^* \xrightarrow{ISC} {}^3\mathrm{ZnPz}^* \quad (1)$$

$$^3\mathrm{ZnPz}^* + {}^3O_2 \rightarrow {}^1O_2 + \mathrm{ZnPz} \quad (2)$$

$$^1O_2 + \mathrm{Subs} \rightarrow \text{Oxidation Products} \quad (3)$$

As close degradation rate of ZnPz(dtnCOOH)$_4$ was compared with iron porphyrazines [17], we still believed that certain reactive radicals might take part in the potocatalytic degradation of RhB with ZnPz(dtnCOOH)$_4$. Indeed, there were also some reported that certain radicals were also formed through the interaction of excited triplet state ($^3$ZnPr* or $^3$ZnPc*) with molecular oxygen [30].

It is reported that fluorescence techniques has been extensively used to detect hydroxyl radicals (HO$^\bullet$) using either coumarin or terephthalic acid, which readily reacts with HO$^\bullet$ to produce highly fluorescent products [31]. Thus coumarin was used to capture hydroxyl radicals, which was produced by the activation of molecular oxygen in the presence of ZnPz(dtnCOOH)$_4$/resin with light irradiation. As shown in insert of Fig. 7, the intensity of fluorescence emission peak increased gradually with the increase of light irradiation time. The results clearly indicated that HO$^\bullet$ was indeed formed during the photocatalytic degradation process of RhB. Based on the relevant work [30], possible mechanism of the production HO$^\bullet$ was proposed as follows (called Type 1 mechanism). The excited triplet state $^3$ZnPz* can produce radicals through interaction with the ground state molecular oxygen [Eq. (1)] to produce $O_2^{\bullet-}$. The $^3$ZnPz* species also interacts with the substrate molecule generating radical ions [Eq. (2)], which then further forms $O_2^{\bullet-}$ [Eq. (3)]. $O_2^{\bullet-}$ further capture the hydrogen of the substrate under acidic condition to form $H_2O_2$ [Eq. (5)], which further forms hydroxyl radicals (HO$^\bullet$) [Eq. (6)]. The latter subsequently afford oxidation of the substrate by Type I mechanism.

$$^3\mathrm{ZnPz}^* + O_2 \rightarrow \mathrm{ZnPz}^{\bullet+} + O_2^{\bullet-} \quad (1)$$

$$^3\mathrm{ZnPz}^* + \mathrm{Subs} \rightarrow \mathrm{ZnPz}^{\bullet-} + \mathrm{Subs}^{\bullet+} \quad (2)$$

$$\mathrm{ZnPz}^{\bullet-} + O_2 \rightarrow \mathrm{ZnPz} + O_2^{\bullet-} \quad (3)$$

$$\mathrm{ZnPz}^{\bullet+} + \mathrm{ZnPz}^{\bullet-} \rightarrow 2\mathrm{ZnPz} \quad (4)$$

$$O_2^{\bullet-} \xrightarrow[\text{Subs-H}]{\mathrm{H}^+} H_2O_2 + \mathrm{Subs}^\bullet \quad (5)$$

$$H_2O_2 \rightarrow 2\mathrm{HO}^\bullet \quad (6)$$

$$\mathrm{Subs} \xrightarrow{\mathrm{HO}^\bullet} \text{Oxidation products} \quad (7)$$

The ZnPz$^{\bullet+}$ species in [Eq. (1)] is a key intermediate. As described above, the central Zinc could not transfer the electrons to molecular oxygen. Therefore, the electron transfer must be promoted by the macroporphyrazine ligand, most probably caused by the electron rich sulfur atoms in the ligand of ZnPz. The above fact was demonstrated by the cyclic voltammetry (CV) of ZnPz(dtnCOOH)$_4$. The solution redox property of ZnPz(dtnCOOH)$_4$ complex 7 were studied using cyclic voltammetry (CV) on a Pt electrode in DMF. Sesalen's group considered that the complexes formed from first-row transition metal with porphyrine, phthalocyanine or porphyrazine due to the fact that the "*d*" electrons of the complexes may occupy the orbital energy level between the HOMO and LUMO of the porphyrine, phthalocyanine, or porphyrazine rings [32]. Therefore, the first oxidation and the first reduction processes should occur on the metal center in the metal complexes only for Mn, Fe and Co derivatives in which valence state of the central metal could be changed, otherwise would occur on the macroporphyrazine ligand. The cyclic voltammogram of the ZnPz(dtnCOOH)$_4$ 7 (solid line) and its free base (dot line) are shown in Fig. 6. According to above discussion, the first oxidation peak reflects the ability of the compound to donate first electron. The lower first oxidation peak O1 (1.35 V) of its free base is from high charge density of sulfur element in their ligand. Moreover, the first oxidation peak O1′ (1.21 V) of ZnPz(dtnCOOH)$_4$ 7 observably to decrease indicates the zinc ion to make the charge density of sulfur element of the ligand shift to the center, so easy to donate electron.

The fluorescent intensities at different pH values were also tested and the results were shown in Fig. 7. It was noted that the

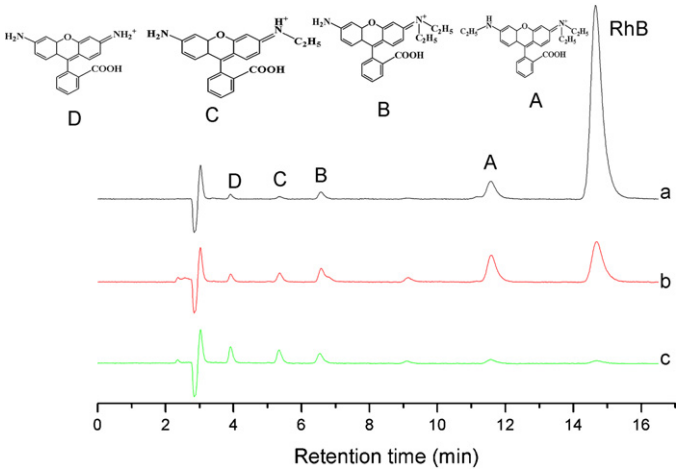


**Fig. 8.** Typical HPLC chromatogram of the degradation products during potocatalytic degradation RhB process. (a) 1 h; (b) 6 h; (c) 12 h.

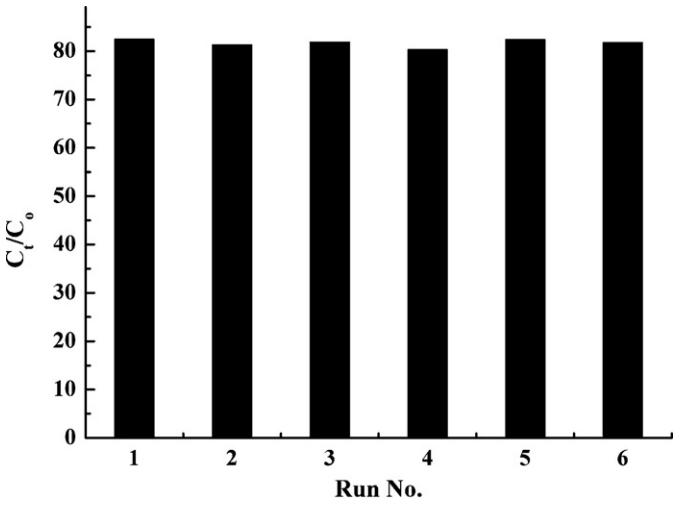


**Fig. 9.** Recycle experiments of the catalyst ZnPz(dtn-COOH)$_4$/resin for the potocatalytic degradation of RhB at pH 3.

fluorescent intensity at pH 3 was much stronger than those at pH 6.86 and 9.18. As showing in the radical mechanism described above, hydroxyl radicals (HO•) was readily to be formed under acidic conditions. Thus, the highest RhB degradation ratio was achieved at pH 3. At the same time, it was noted that hydroxyl radicals at pH 9.18 and 6.18 were almost kept constant at low lever, indicating that hydroxyl radicals were not readily formed in neutral and alkaline aqueous solution. However, the degradation ratio of RhB reached 54% and 34% at pH 9.18 and 6.18, respectively. It indicated that the popular mechanism which involves $^1O_2$ was still taken part in the degradation of RhB, but in acidic condition, both Type I and Type II mechanisms which involves $^1O_2$ and HO• were involved in the degradation of RhB. If the degradation ratio of 34% in neutral solution was considered as a pure oxidation from $^1O_2$, the difference 48% between the degradation ratio of 82% in acidic solution and 34% in neutral solution should be the efficiency of oxidation degradation by radicals such as HO•. It could be concluded that the degradation of RhB was mainly aroused by radicals such as HO• in the presence of the catalyst ZnPz(dtnCOOH)$_4$/resin and acid solution under visible light.

### 3.6. HPLC analysis of degradation products

HPLC spectrum was then employed to further study the photooxidation degradation products, showing in Fig. 8. The HPLC chromatogram of the degradation products from RhB was similar with the previous results of Horikoshi group [33]. At 1 h, Four main components N,N-diehyl-N-ethyl-rhodamine (product A, retention time: 11.6 min), N,N-diethyl-rhodamine (product B, retention time: 6.6 min), N-ethyl-rhodamine (product C, retention time: 5.4 min), rhodamine (product D, retention time: 3.9 min) were detected by HPLC using a reversed-phase C18 column at 500 nm. Seeing from the HPLC chromatogram, it was found that RhB was rapidly degraded and no RhB was remained after 12 h. The amount of product A was increased from 1 h to 6 h, and then it decreased gradually. However, the amount of other degradation products such as B, C, D, which were formed from the further de-ethylation of product A were almost stable during the degradation process. These results indicated that product A was the main intermediate during the degradation of RhB. As far as RhB degradation mechanism, two mechanisms were broadly accepted [33]. One possible mechanism was that four ethyl groups were gradually released, and rhodamine (product D) was ultimately degraded by reactive oxidizing species. The typical characteristic of this mechanism was that the clear hypsochromic shifts of the maximum absorption of RhB were observed, due to the de-ethylation products B, C, D have much shorter wavelength. The other possible mechanism was N,N-diehyl-N-ethyl-rhodamine (product A) was the main intermediate, which was directly cleaved by reactive oxidizing species. In this study, product A was detected to be the main intermediate, and hypsochromic shifts of the maximum absorption of RhB were not clearly observed. Thus, the most probable mechanism of RhB degradation in this study was that N,N-diehyl-N-ethyl-rhodamine was the main intermediate, which was then cleaved to small molecule by reactive oxidizing species such as hydroxyl radicals (HO•).

### 3.7. Reusability and stability experiment

Finally, the reusability and stability of ZnPz(dtn-COOH)$_4$/resin was evaluated. After the degradation of RhB was finished with the use of fresh catalyst at pH 3, the used catalyst was collected by filtration, washed with water several times until the filter liquor to be neutral, and dried at 60 °C in vacuum overnight. Then, the recovered catalyst was added into a fresh solution of RhB and the second cycle was carried out under the same conditions. These steps were repeated for five times, and the degradation results were shown in Fig. 9. It was found that the degradation ratios of RhB were almost kept stable around 80%. Therefore, this novel biomimetic photocatalyst ZnPz(dtn-COOH)$_4$/resin can be reused several times without losing its catalytic activity, being favorable to the potential application in practical wastewater treatment.

## 4. Conclusion

In this study, a novel biomimetic photocatalyst ZnPz(dtn-COOH)$_4$ was successfully synthesized by the template method. The ZnPz(dtn-COOH)$_4$ supported on Amberlite CG-400 resin showed good photocatalytic performance for activating molecular oxygen under visible light irradiation, and RhB could be effectively degraded by about 82% for 12 h at pH 3. Through fluorescence techniques, more hydroxyl radicals were produced at pH 3, both Type I and Type II mechanisms were involved in the degradation of RhB, which was mainly aroused by radicals such as HO•. Moreover, the most probable mechanism of RhB degradation in this study was that N,N-diehyl-N-ethyl-rhodamine was the main intermediate, which was then cleaved to small molecule by reactive oxidizing species. In addition, the catalyst could be used five times without losing its catalytic activity. This work introduces a novel, promising, biomimetic

and green photooxidation catalyst for the degradation of organic pollutants.

## Acknowledgements

This work was finally supported by the National Natural Sciemce Foundation of China (Nos. 20977115, and 21272281), and the Innovative Research Team Foundation of Hubei Province (2010CDA068).

## References

[1] E. Forgacs, T. Cserhati, G. Oros, Environment International 30 (2004) 953–971.
[2] A. Panniello, M.L. Curri, D. Diso, A. Licciulli, V. Locaputo, A. Agostiano, R. Comparelli, G. Mascolo, Applied Catalysis B: Environmental 121 (2012) 190–197.
[3] A. Bhatnagar, V.J.P. Vilar, C.M.S. Botelho, R.A.R. Boaventura, Environmental Technology 32 (2011) 231–249.
[4] C.A. Orge, J.J.M. Orfao, M.F.R. Pereira, Applied Catalysis B: Environmental 102 (2012) 539–546.
[5] C.C. Chen, W.H. Ma, J.C. Zhao, Chemical Society Reviews 39 (2010) 4206–4219.
[6] A.L. Eusebi, A. Massi, E. Sablone, M. Santinelli, P. Battistoni, Water Science and Technology 65 (2012) 721–727.
[7] S. Harendra, D. Oryshchyn, T. Ochs, S. Gerdemann, J. Clark, C. Summers, Industrial and Engineering Chemistry Research 50 (2011) 10335–10343.
[8] F.J. Benitez, J.L. Acero, F.J. Real, C.J. Garcia, Chemical Technology & Biotechnology 84 (2009) 1883–1893.
[9] M.L. Marin, L. Santos-Juanes, A. Arques, A.M. Amat, M.A. Miranda, Chemical Reviews 112 (2012) 1710–1750.
[10] N.U. Silva, T.G. Nunes, M.S. Saraiva, M.S. Shalamzari, P.D. Vaz, O.C. Monteiro, C.D. Nunes, Applied Catalysis B: Environmental 113 (2012) 180–191.
[11] J.Y. Jing, M.H. Liu, V.L. Colvin, W.Y. Li, W.W. Yu, Journal of Molecular Catalysis A: Chemical 351 (2011) 17–28.
[12] A. Thibon, V. Jollet, C. Ribal, K. Senechal-David, L. Billon, A.B. Sorokin, F. Banse, Chemistry A European Journal 18 (2012) 2715–2724.
[13] J.R. Lindsay Smith, in: R.G. Sheldon (Ed.), Metalloporphyrins in Catalytic Oxidations, Marcel Dekker, New York, NY, 1994 (Chapter 11).
[14] X. Tao, W.H. Ma, J. Li, Y.P. Huang, J.C. Zhao, J.C. Yu, Chemistry Communications 1 (2003) 80–81.
[15] C.M. Che, V.K.Y. Lo, C.Y. Zhou, J.S. Huang, Chemical Society Reviews 40 (2011) 1950–1975.
[16] E.S. Taraymovich, A.B. Korzhenevskii, Y.V. Mitasova, R.S. Kumeev, O.I. Koifman, P.A. Stuzhin, Journal of Porphyrins and Phthalocyanines 15 (2011) 54–65.
[17] C.J. Yang, J. Sun, K.J. Deng, D.Y. Wang, Catalysis Communications 9 (2008) 321–326.
[18] J.F. Tang, L.Q. Chen, J. Sun, K.L. Lv, K.J. Deng, Inorganic Chemistry Communications 13 (2010) 236–239.
[19] A. Maldotti, L. Andreotti, A. Molinari, S. Borisov, V. Vasil'ev, Chemistry A European Journal 7 (2001) 3564–3571.
[20] H.E. Simmons, D.C. Blomstrom, R.D. Vest, Journal of the American Chemical Society 844 (1964) 4756–4771.
[21] C.F. van Nostrum, R.J.M. Nolte, Chemical Communications (1996) 2385–2392.
[22] A.E. Pullen, C. Faulmann, P. Cassoux, European Journal of Inorganic Chemistry 38 (1999) 269–276.
[23] S.I. Hachiya, A.S. Cook, B.G. Williams, A.G. Montalban, A.G.M. Barrett, B.M. Hoffman, Tetrahedron 56 (2000) 6565–6569.
[24] E. Gonca, Y. Koseoglu, B. Aktas, A. Gül, Polyhedron 23 (2004) 1845–1849.
[25] D. Dhami, D. Phillips, Journal of Photochemistry and Photobiology A 100 (1996) 77–84.
[26] J. Zhao, T. Wu, K. Wu, K. Oikawa, H. Hidaka, N. Serpone, Environmental Science and Technology 32 (1998) 2394–2400.
[27] T. Wu, G. Liu, J. Zhao, H. Hidaka, N. Serpone, Journal of Physical Chemistry B 102 (1998) 5845–5851.
[28] Y.J. Li, W. Chen, Catalysis Science & Technology 1 (2011) 802–809.
[29] R. Bonnett, Chemical Society Reviews 24 (1995) 19–33.
[30] I. Rosenthal, E. Ben-Hur, International Journal of Radiation Biology 67 (1995) 85–91.
[31] K. Ishibashi, A. Fujishima, T. Watanabe, K. Hashimoto, Electrochemistry Communications 2 (2000) 207–210.
[32] B.S. Sesalan, A. Koca, A. Gül, Dyes Pigments 79 (2008) 259–264.
[33] S. Horikoshi, A. Saitou, H. Hidaka, Environmental Science and Technology 37 (2003) 5813–5822.